NIH Public Access
Author Manuscript
Acta Biomater. Author manuscript; available in PMC 2014 May 01.

Published in final edited form as:
Acta Biomater. 2013 May ; 9(5): 6563–6575. doi:10.1016/j.actbio.2013.01.004.

The influence of scaffold material on chondrocytes in inflammatory conditions

Heenam Kwon[1,2], **Lin Sun**[3], **Dana M. Cairns**[1,2], **Roshni S. Rainbow**[2], **Rucsanda Carmen Preda**[3], **David L. Kaplan**[1,3,4], and **Li Zeng**[1,2,5,*]

[1]Program in Cellular, Molecular and Developmental Biology, Sackler School of Graduate Biomedical Sciences, Tufts University School of Medicine, 136 Harrison Avenue, Boston, MA 02111, USA

[2]Department of Anatomy and Cellular Biology, Tufts University School of Medicine. 136 Harrison Avenue, Boston, MA 02111

[3]Department of Chemical and Biological Engineering, Tufts University, 4 Colby Street, Medford, MA 02155

[4]Department of Biomedical Engineering, Tufts University, 4 Colby Street, Medford, MA 02155

[5]Department of Orthopaedic Surgery, Tufts Medical Center, 800 Washington Street, Boston, MA 02111, USA

Abstract

Cartilage tissue engineering aims to repair damaged cartilage tissue in arthritic joints. As arthritic joints have significantly higher levels of pro-inflammatory cytokines (such as IL-1β and TNFα that cause cartilage destruction, it is critical to engineer stable cartilage in an inflammatory environment. Biomaterial scaffolds constitute an important component of the microenvironment for chondrocytes in engineered cartilage. However, it remains unclear how scaffold material influences the response of chondrocytes seeded in these scaffolds under inflammatory stimuli. Here, we compared the response of articular chondrocytes seeded within three different polymeric scaffolding materials (silk, collagen and polylactic acid (PLA)) to IL-1β and TNFα. These scaffolds have different physical characteristics and yielded significant differences in the expression of genes associated with cartilage matrix production and degradation, cell adhesion and cell death. Silk and collagen scaffolds released pro-inflammatory cytokines faster and had higher uptake water abilities than PLA scaffolds. Correspondingly, chondrocytes cultured in silk and collagen scaffolds maintained higher levels of cartilage matrix than those in PLA, suggesting that these biophysical properties of scaffolds may regulate gene expression and response to inflammatory stimuli in chondrocytes. Based on this study, we concluded that selecting the proper scaffolding material will aid in the engineering of more stable cartilage tissues for cartilage repair; and that silk and collagen are the more optimal scaffolds in supporting the stability of 3D cartilage under inflammatory conditions.

© 2013 Acta Materialia Inc. Published by Elsevier Ltd. All rights reserved.

*Corresponding author: Li Zeng (li.zeng@tufts.edu; phone: 617-636-2107, fax: 617-636-3676) .

Publisher's Disclaimer: This is a PDF file of an unedited manuscript that has been accepted for publication. As a service to our customers we are providing this early version of the manuscript. The manuscript will undergo copyediting, typesetting, and review of the resulting proof before it is published in its final citable form. Please note that during the production process errors may be discovered which could affect the content, and all legal disclaimers that apply to the journal pertain.

NIH-PA Author Manuscript
NIH-PA Author Manuscript
NIH-PA Author Manuscript

NIH-PA Author Manuscript

NIH-PA Author Manuscript

NIH-PA Author Manuscript

Keywords

cartilage matrix production; scaffold; pro-inflammatory cytokines; cytokine release; water uptake

1 Introduction

Arthritis is the leading debilitating joint disease caused by the destruction of joint cartilage and is accompanied by inflammation and pain [1-3]. However, articular cartilage has a limited regenerative capacity *in vivo*, and optimal treatments for arthritis are still lacking. Cartilage tissue engineering has emerged as a potential therapeutic option for cartilage repair [4-7], which generally involves the reconstruction of three-dimensional (3D) tissues by seeding chondrocytes into natural or synthetic scaffolds, although scaffold-free cultures have also been explored for tissue engineering applications [5, 8, 9]. *In vitro* grown cartilage constructs can then be transplanted into the host joint to resume function. In addition to cell-loaded scaffolds, cell-free materials may be placed in the cartilage defects to harbor migrating cells and provide mechanical support to enhance cartilage repair [10-12]. Scaffold architecture has the advantages of providing further mechanical support and open conduits for mass transfer of oxygen and nutrients, thus constituting an important part of the chondrocytes' microenvironment [5].

In selecting suitable scaffolding material for cartilage constructs, it is critical to consider the biocompatibility and mechanical strength of the material, as well as its ability to support maximum cartilage matrix production [13-15]. As bioengineered cartilage constructs will be eventually transplanted into arthritic joints that have elevated levels of pro-inflammatory cytokines that destroy cartilage, it is especially important to select scaffolds that support the stability of bioengineered cartilage in an inflammatory environment [4, 16-18]. Multiple studies have shown that scaffolds made from various biomaterials have different surface features and physical characteristics that affect cell growth, cell attachment and matrix production [19-21]. However, little is known about how scaffold material may influence the homeostasis of the chondrocytes seeded within the scaffolds under inflammatory stimuli.

We hypothesized that the scaffold's biophysical and chemical properties regulate the expression of cartilage matrix and degradation-related genes in chondrocytes in the presence of pro-inflammatory cytokines. To test this hypothesis, we conducted a thorough investigation of cell morphology and gene expression in chondrocytes cultured in scaffolds derived from different biomaterials under the treatment of pro-inflammatory cytokines, IL-1β and TNFα. We selected porous scaffolds derived from three different degradable and polymeric materials, silk, collagen, and poly-lactic acid (PLA), as they are all widely used for tissue engineering [22-25]. As a natural material, collagen has adequate biocompatibility, biodegradability and a low immunogenic profile, but does not provide strong mechanical support [5, 26-28]. Silk, a natural material prepared from silk fibroin of the silkworm, also has adequate biocompatibility. In addition, silk has impressive biomechanical properties [22, 25, 29-32]. Polylactic acid (PLA), on the other hand, is a synthetic polymeric material whose properties, such as mechanical strength, degradation rate and dimension can all be easily controlled [5]. However, PLA material has been reported to provoke a higher inflammatory response in the host than silk [28].

In this study, we found that primary bovine articular chondrocytes (BACs) when cultured within silk, collagen and PLA scaffolds, exhibited different cellular morphologies and expressed significantly different levels of cartilage matrix components and destruction genes. Furthermore, we characterized the biophysical properties of the scaffolds in terms of their abilities to release pro-inflammatory cytokines and uptake water, which may influence

NIH-PA Author Manuscript

NIH-PA Author Manuscript

NIH-PA Author Manuscript

the biochemical responses of chondrocytes under inflammatory conditions. Together, the study strongly suggests that scaffolding material plays an important role in the microenvironment of engineered cartilage, and regulates the response of chondrocytes under inflammatory conditions.

2. Materials and methods

2.1. Scaffold preparation

Three-dimensional (3D) scaffolds derived from collagen (bovine derived type I and III collagens), and polylactic acid (PLA) were purchased from BD Biosciences (San Jose, CA, USA). Average pore sizes of collagen and PLA scaffolds were 100-200 μm and dimensions were 5mm × 3mm (diameter × height), according to manufacturer's specifications.

Silk scaffolds were prepared as previously described [27, 33]. Briefly, cocoons of *Bombyx mori* were boiled for 30 minutes in an aqueous solution of 0.02M Na_2CO_3 and rinsed with distilled water to eliminate sericin. Purified silk fibroin was solubilized in 9.3M LiBr solution and dialyzed against distilled water. The resulting silk fibroin solution was lyophilized and dissolved in hexafluoroisopropanol (HFIP) to obtain a 10% (w/v) silk solution. To create the desired pore size, 1 mL of the 10% silk-HFIP solution was added to 3.4 g of NaCl with a particle size of 106-212 μm in disk-shaped containers. The containers were tightly covered and left in the fume hood for 1-2 days for the silk-HFIP solution to evenly mix with the salt particles. The solvent was then evaporated for 3 days at room temperature. The scaffolds were treated with methanol for 1-2 days, and then the methanol was evaporated and the scaffolds were immersed in distilled water for additional 2 days to extract the salt particles. Porous silk scaffolds were then cut into disks with the same dimension as collagen and PLA scaffolds (5mm×3mm (diameter× height)) and autoclaved for cell seeding. The pore sizes of these scaffolds were confirmed by Image J analysis of the SEM images (silk: 170 ± 34μm; collagen: 165±31μm; and PLA: 184±57μm) [34, 35]. The porosities measured by Image J analysis on SEM images were: Silk: 51.6±8.5%; collagen: 57.1±4.3%; PLA: 53.4±10.4%, using an established protocol [36-39].

2.2. Isolation of bovine articular chondrocytes

Bovine articular chondrocytes (BACs) were isolated as previously described [40, 41]. Articular cartilage from all surfaces of a bovine cadaver knee joint (Research 87, Inc. Pleasant Lane, Boylston, MA, USA, (508) 869-0100) was dissected and transferred to a tube containing PBS and 10% penicillin/streptomycin. For dissociation of articular chondrocytes from cartilage matrix, minced cartilage pieces (12-15cm^3 total in volume) were treated with 20ml of 1mg/ml hyaluronidase solution (Sigma, St. Louis, MP, USA) for 15min followed by treatments with20ml of 0.25% trypsin solution (Sigma) for 30min, and 20ml of 2mg/ml collagenase solution (Sigma) for approximately 15h at 37°C. For removal of any undigested cartilage to obtain a single cell suspension, isolated chondrocytes were passed through a 40μm strainer twice. The single cell population was resuspended in cell freezing medium (90% Fetal bovine serum (FBS) (Thermo Scientific HyClone, New Zealand), 10% DMSO (Sigma)), and stored in liquid nitrogen until experimentation. Cell viability was determined using the standard trypan blue staining protocol, where positive staining indicated cell death when isolated cells were mixed with trypan blue solution (Sigma). At isolation, cell viability was 97.2±2.4%. After freezing and thawing, cell viability was 73.7±4.3%. The viability of thawed cells after three days of culturing was 99.1±4.5%. The purity of the chondrocytes was confirmed by immunocytochemistry for cartilage marker Sox9, which showed 99% of the cells were Sox9-positive (Supplemental Figure 1). Only passage 0 cells (P0) were used for all experiments.

NIH-PA Author Manuscript

NIH-PA Author Manuscript

NIH-PA Author Manuscript

2.3. Cell seeding and 3D culturing

To prepare for cell seeding, scaffolds derived from silk, collagen, and PLA were pre-wetted with sterile DMEM (Gibco, Carlsbad, CA, USA) overnight. Scaffolds were then removed from media and chondrocytes were seeded into scaffolds at a seeding density of 5×10^4 cells/scaffold. This cell density would allow easy access of all chondrocytes to both the scaffolds and pro-inflammatory cytokines. We have found that RNA yield from harvested chondrocytes at this seeding density rose consistently over the 16 day culture period (refer to Supplemental Information), suggesting that cells were viable and proliferating. Based on the dimension of the scaffolds, we calculated our initial seeding density to be 3.1×10^3 cells/mm^3. Taken into the consideration of cell proliferation over the culture period, the cell density in the scaffolds should be comparable to the cellularity of the adult native cartilage tissue (15×10^3 cells/mm^3) [42]. After seeding, cell-loaded scaffolds were placed in a humidified tissue culture incubator at 37°C with 5% CO_2 for 2 hours to allow for cell attachment. Cell-loaded scaffolds were then cultured in fresh DMEM containing 10% FBS and 1% Antibiotic-antimycotic (Gibco) for 8 days and 16 days on a shaker (5-6rpm, 6hr/day) in a tissue culture incubator. Three experimental groups were included in each independent experiment: control, 10ng/ml of IL-1β, and 10ng/ml of TNFα (Peprotech, Rocky Hill, NJ, USA). Medium was changed every 2-3days.

2.4. Scanning electron microscopy (SEM)

Cell-loaded scaffolds were fixed in 2.5% glutaraldehyde in 0.1M sodium cacodylate buffer (pH=7.4) at 4°C overnight. Samples (two scaffolds from two independent experiments from each condition) were then treated with 1% osmium tetroxide for 1hr, dehydrated in ethanol, and subsequently dried on an Edwards Auto 306 Vacuum Evaporator. The samples were then cross-sectioned and sputter coated with palladium-gold. Chondrocytes grown inside the scaffolds were observed using an ISI DS130 scanning electron microscope at the Tufts Imaging Facility.

2.5. Histological stainings

After 16 days of culture, cell-loaded scaffolds were fixed in 10% neutral-buffered formalin for histological evaluation. Silk and collagen scaffolds were embedded in paraffin while PLA scaffolds were embedded in OCT for frozen sectioning as PLA melts in xylene during the paraffinization process. The embedded samples were sectioned at 10μm thickness and were subsequently processed and stained with hematoxylin and eosin (H&E) and toluidine blue using standard protocols. Image J software was used to quantify chondrocyte dimensions from images of H&E staining as well as the intensities of toluidine blue in toluidine blue-stained slides using established protocols [43]. Two different scaffolds from two independent experiments per treatment and time point were examined by H&E and toluidine blue staining analysis. For each scaffold and each staining, 12-20 sections were examined.

2.6. RNA isolation and real-time RT-PCR

Total RNA from cell-loaded scaffolds was obtained using the RNeasy mini kit (Qiagen, Hilden, Germany), according to the manufacturer's protocol. Three independent experiments were performed. For each experiment, at least three independent samples per treatment per time point were used for RT-PCR analysis. The RNA was reverse transcribed into cDNA using the M-MLV reverse transcriptase kit (Invitrogen), random primers (Invitrogen) and dNTPs (New England BioLabs, MA, USA). All cDNA was stored at −20°C for later analyses. For RNA and cDNA yield, refer to Supplemental Information. For each RT-PCR reaction, 7ng of cDNA was mixed with gene specific primers and SYBR® green SuperMix (Quanta Bioscience, Inc., Gaithersburg, MD, USA) and loaded on the iQ5 Real

NIH-PA Author Manuscript

NIH-PA Author Manuscript

NIH-PA Author Manuscript

time PCR Thermocycler and Detection system (BioRad, Hercules, CA, USA) and analyzed by iQ5 optical system software. For PCR primers, refer to Supplemental Information (Supplemental Table 1). All transcript levels were normalized to glyceraldehyde-3-phosphate dehydrogenase (GAPDH) level.

2.7. Analysis of cytokine release from the scaffolds into the medium

0.1ng, 1ng, or 10ng of pro-inflammatory cytokines, IL-1β or TNFα (Peprotech) were loaded onto pre-wetted scaffolds in a volume of 10μl. For each material, 3-6 scaffolds per treatment per time point were used. Loaded scaffolds were incubated for 6 hr at room temperature, immersed into 1ml of culture medium, and then placed in a humidified tissue culture incubator at 37°C with 5% CO_2. The scaffolds were removed and transferred into fresh medium at each time point (t=10min, 1hr, 1d, 3d, and 5d). At every time point, medium conditioned by the scaffolds was collected and stored in −80°C for later analysis. The initial loading amount and concentrations of pro-inflammatory cytokines at all time points present in the collected media samples were quantified using ELISA (Quantikine; R&D Systems, Minneapolis, MN, USA). Percent release was calculated as the ratio of the amount of cytokines in the medium to the initial amount of cytokines loaded onto the scaffolds. Percent cumulative release was calculated as the ratio of cumulative amount of cytokines in the medium at each time point (i.e. sum cytokine amount at each time point and all prior time points) to the initial amount of cytokines loaded onto the scaffolds.

2.8. Analysis of water uptake abilities of the scaffolds

The water uptake abilities of silk, collagen, and PLA scaffolds were determined using a previously established protocol [22]. For each material, 3-6 scaffolds/treatment were used. Scaffolds were immersed in distilled water for 24 hours at room temperature. The wet weight of the scaffolds (W_{wet}) was measured after removing excess water from the scaffolds. The scaffolds were then dried in an oven at 65°C overnight and the weight of dried scaffolds (W_{dry}) were then measured. The water uptake (%) values were obtained using the following formula:

$$\text{Water uptake}\,(\%) = \left[\left(W_{wet} - W_{dry}\right)/W_{wet}\right] \times 100$$

2.9. Statistical analysis

Three independent experiments were performed. All data were presented as mean ± SD (standard deviation) with a minimum of n=3. For determination of statistical differences among the materials in a specific condition, one-way ANOVA with post-hoc Tukey test (GraphPad Prism; http://www.graphpad.com) was used. For determination of statistical differences among the different conditions of cytokine treatment in different scaffolds, two-way ANOVA with Bonferroni post test was used. Details of reference factors for each type of experiment were presented as Supplemental Information. $p < 0.05$ was considered statistically significant.

3. Results

3.1. Silk, collagen and PLA scaffolds support different chondrocyte morphologies under IL-1β and TNFα treatments

To evaluate the effect of scaffolding material on the morphology of chondrocytes under inflammatory stimuli, we performed scanning electron microscopy (SEM) analysis. We found that all scaffolds differed in their surface roughness (Fig. 1A). PLA scaffolds had the smoothest surfaces, while collagen scaffolds had the roughest (Fig. 1A). Although all

NIH-PA Author Manuscript

NIH-PA Author Manuscript

NIH-PA Author Manuscript

scaffolds had the same pore sizes, pores in the PLA and silk scaffolds were more homogeneously distributed than those in the collagen scaffolds, which are lined with collagen fibrils (Fig. 1A). Furthermore, the shapes of the pores differed slightly for each scaffold. Pores of silk and PLA scaffolds were round, while those of collagen scaffolds were sometimes more oval-shaped (Fig. 1A). After culturing for 16 days in these scaffolds, regardless of the material, chondrocytes were attached to the surfaces of the scaffolds and evenly distributed (Fig. 1B and 1C).

3.2. Silk, collagen and PLA scaffolds support different cartilage gene expression in chondrocytes under IL-1β and TNFα treatments

3.2.1. Cartilage matrix deposition—To investigate the effect of scaffold material on articular chondrocyte homeostasis under inflammatory conditions, we evaluated cartilage matrix production using histological analysis. We first performed H&E staining on sections of cell-loaded silk, collagen and PLA scaffolds. We found that chondrocytes grown in silk and collagen scaffolds tended to be more compact, while those grown in PLA scaffolds appeared larger (Fig. 2A). To provide a more quantitative analysis on cell sizes, we calculated the areas of chondrocytes shown in these sections, and found that cells in PLA scaffolds indeed had larger surface areas than those in silk and collagen scaffolds (Fig. 2B). Histological analysis using toluidine blue indicates that chondrocytes cultured in silk and collagen scaffolds had more intense toluidine blue staining than those cultured in PLA-scaffolds, suggesting the presence of a higher level of total glycosaminoglycans (GAGs) in the silk and collagen scaffolds (Fig. 2A) [44]. In the presence of IL-1β and TNFα, staining surrounding the chondrocytes cultured in silk and collagen scaffolds became less intense, while those in the PLA scaffolds remained at lower levels (Fig. 2A). Quantification of staining intensities using the Image J software indicated that PLA scaffolds supported lower cartilage matrix production in control or IL-1β and TNFα treatment conditions than silk and collagen scaffolds (Fig. 2D), which is consistent with the flatter cell morphology of the chondrocytes grown in PLA scaffolds and supports the notion that flatter cell morphology is correlated with less cartilage matrix production [45].

3.2.2. Cartilage matrix-related genes—To determine whether the differences in cartilage matrix production in chondrocytes grown in silk, collagen and PLA scaffolds were due to differed transcriptional levels of genes controlling cartilage matrix production, degradation and cell survival, we performed qRT-PCR analysis on cultures of day 8 and day 16. First, we evaluated the expression of cartilage matrix genes collagen II, collagen IX and aggrecan. Collagen II and collagen IX are the signature collagens uniquely expressed in the cartilage tissues, while aggrecan is the major proteoglycan component in the extracellular matrix (ECM), and consists of the aggrecan core protein and the GAGs that bind to it. Thus aggrecan expression is expected to reflect the overall GAG content [46, 47]. On the other hand, Sox9 is a transcription factor that serves as a master regulator of chondrogenesis by directly binding to the collagen II and aggrecan promoters [48, 49]. At day 8, there were no significant differences in Sox9 expression in chondrocytes grown in the three types of scaffolds under normal conditions (Fig. 3A). However, the expression of collagen II, collagen IX and aggrecan was already significantly higher in chondrocytes seeded in silk scaffolds as compared to collagen and PLA in control samples (Fig. 3A). In the presence of IL-1β, chondrocytes grown in silk scaffolds expressed significantly higher levels of Sox9, collagen II and collagen IX than those in PLA scaffolds at day 8 (Fig. 3A). Upon TNFα treatment, silk scaffolds still supported a higher level of collagen IX expression than PLA scaffolds at day 8 (Fig. 3A). By 16 days of culture, all cartilage matrix-related genes were further downregulated by pro-inflammatory cytokines, however, chondrocytes seeded in silk and collagen scaffolds continued to show an overall higher expression in cartilage matrix

NIH-PA Author Manuscript

NIH-PA Author Manuscript

NIH-PA Author Manuscript

genes than those in PLA scaffolds (Fig. 3B). We did not perform a time course longer than day 16, as cartilage matrix gene expression was already reduced to a minimum level.

3.2.3. Chondrocyte hypertrophy and dedifferentiation genes—We then evaluated the expression of chondrocyte hypertrophy markers collagen X and alkaline phosphatase (ALP) (Fig. 4). In addition, we assayed collagen I expression, which should be upregulated if the chondrocytes are de-differentiated (Fig. 4). Our data showed that the levels of collagen X and collagen I were similar in different scaffolds, in the absence or presence of IL-1β and TNFα, at both day 8 and day 16. However, ALP was generally strongly induced by TNFα, but not IL-1β (Fig. 4). These data suggest that scaffold material did not affect the status of hypertrophy and de-differentiation in these articular chondrocytes.

3.2.4. Chondrocyte-degradation-related genes—It is well established that metalloproteinases that degrade collagens and aggrecan, including MMP3, MMP13 and ADAMTS4, are induced by pro-inflammatory cytokines [50]. Our results indicated that scaffolds of different materials elicited different responses with respect to the various matrix-degrading enzymes and at various time points to IL-1β and TNFα. At day 8, significantly higher levels of MMP3, MMP13 and ADAMTS4 were induced by IL-1β in chondrocytes grown in silk scaffolds than in those grown in collagen and PLA scaffolds, while there was no difference in TNFα–treated samples (Fig. 5A). Interestingly however, after 16 days of culture, while there were no differences in between scaffolds under control conditions, MMP13 expression was significantly lower in chondrocytes cultured in silk and collagen scaffolds than those in PLA scaffolds under IL-1β or TNFα treatment (Fig. 5B).

3.2.5. Cell adhesion-related genes—Different scaffolding materials have different surface chemistry properties and rigidity, which may affect cell adhesion and may in turn influence gene expression [19-21]. Thus, we evaluated the expression of integrins and cadherins, which are mediators of cell adhesion [51-53]. Both α1 and β1 integrins are highly expressed in the chondrocytes and bind to collagens in cartilage ECM [51]. On the other hand, N-cadherin, which normally mediates condensation during chondrocyte differentiation, exhibits diminished expression in differentiated chondrocytes [54-59]. We found that chondrocytes grown in PLA scaffolds expressed significantly higher levels of α1-integrin than those in silk scaffolds at day 8 upon IL-1β treatment (Fig. 6A) and at day 16 in all conditions (Fig. 6B). In addition, N-cadherin was much more strongly induced in chondrocytes by TNFα than IL-1β (Fig. 6A and 6B). Given that chondrocytes in PLA scaffolds exhibited a more flattened morphology (Fig. 2), this result is consistent with another study that showed that increased expression of α1-integrin is associated with an elongated rather than round chondrocyte cell shape [45].

3.2.6. Cell death-related genes—We next evaluated the expression of caspases and inducible nitric oxide synthase (iNOS), which are mediators of apoptosis and induced by pro-inflammatory cytokines [60]. We found that caspase 3 was more strongly induced by IL-1β and TNFα in chondrocytes grown in collagen and PLA scaffolds than in silk scaffolds at day 16 (Fig. 7). In contrast, there were no significant differences in caspase 8 expression in chondrocytes grown in scaffolds of different materials throughout the culture periods (Fig. 7). On the other hand, iNOS was expressed at higher levels in chondrocytes grown in silk scaffolds than in collagen and PLA scaffolds (Fig. 7). Additionally, while TNFα strongly induced caspase 8 expression, IL-1β preferentially induced iNOS expression, thereby suggesting that IL-1β and TNFα have different effects on these genes (Fig. 7).

NIH-PA Author Manuscript

NIH-PA Author Manuscript

NIH-PA Author Manuscript

3.3. Silk, collagen and PLA scaffolds have different cytokine release properties and water uptake capacities

To understand the possible underlying mechanisms that cause the differential responses to pro-inflammatory cytokines, we evaluated the following biophysical properties of the three different types of scaffolds.

3.3.1. The ability to release pro-inflammatory cytokines—Our rationale was that higher affinity of the scaffolds for pro-inflammatory cytokines would lead to higher local concentrations of these factors within the cartilage construct, and differences of the cytokine levels in the scaffold may in turn affect cartilage gene expression. Therefore, to investigate how the scaffolds release or retain IL-1β and TNFα, we applied equal amounts of these cytokines to silk, collagen and PLA scaffolds, and then evaluated the amount of cytokines that leached out into the medium. As we were uncertain of the capacity of the scaffolds to adsorb IL-1β or TNFα, we applied three different amounts (0.1ng, 1ng and 10ng) to the scaffolds, placed the scaffolds in the medium, and assayed by ELISA the amount of cytokines leached into the medium at different time points (Fig. 8 and Supplemental Fig. 2). We found that regardless of loading levels, the amount of IL-1β released from silk scaffolds was significantly higher than that from collagen and PLA scaffolds at the initial time point of 10min, as well as at the end of the study (cumulative release) (Fig. 8A and 8B). In contrast, collagen scaffolds maintained a steady release over the first day of the study and had the lowest cumulative release of IL-1β at early time points (Fig. 8A and 8B). The release of TNFα from silk, collagen and PLA scaffolds exhibited a similar trend to that of IL-1β, with silk scaffolds releasing the highest amount of TNFα than other scaffolds (Fig. 8C and 8D). This finding suggests that silk scaffolds may support a microenvironment where there are lower levels of IL-1β and TNFα, a result that may help to explain the higher levels of cartilage matrix gene expression in these scaffolds as compared to PLA scaffolds.

3.3.2. Water uptake ability of the scaffolds—Water uptake ability is known to reflect the hydrophilicity property of the scaffolds [61-63]. Our rationale was that this property could affect the effective cytokine concentrations in the scaffold microenvironment of the chondrocytes and in turn chondrocyte gene expression. Using established protocols [22, 64], we determined that silk and collagen scaffolds have a significantly higher water uptake capacity than PLA scaffolds, suggesting that silk and collagen scaffolds created a more hydrated microenvironment for the chondrocytes (Fig. 8).

4. Discussion

A major goal of cartilage tissue engineering is to repair damaged cartilage tissues caused by mechanical stress and high levels of pro-inflammatory cytokines in arthritic joints. It is clear that the stability of bioengineered cartilage can be compromised by pro-inflammatory cytokine-induced cartilage matrix degradation [65, 66]. Several biochemical factors or reagents, such as IGF-I, PDGF, and Cox-2 inhibitor celecoxib, were shown to possess inhibitory activities to IL-1β-induced matrix reduction in chondrocytes in 2D cultures [67, 68]. In 3D cultures, dexamethasone and MMP inhibitor TIMP-1 demonstrated a protective effect against IL-1α [65, 69]. Interestingly, genipin, a cross-linking reagent, was found to inhibit IL-1α-induced GAG reduction when administered in the culture medium, possibly by stabilizing the ECM [70]. On the other hand, dynamic loading did not alleviate the catabolic effect of IL-1α and IL-1β in the cartilage construct [71]. Since dynamic loading has been widely regarded to enhance cartilage matrix production, this study suggests that matrix production under normal conditions and matrix maintenance under inflammatory conditions are two related but not identical issues [71]. Apart from biochemical factors, very

NIH-PA Author Manuscript

NIH-PA Author Manuscript

NIH-PA Author Manuscript

little is known about the contribution of other components in a 3D cartilage toward inflammatory response.

Scaffolds constitute an important component of the microenvironment for chondrocytes in bioengineered cartilage. Selecting the optimal scaffolds, together with supplementing the optimal biochemical factors in the culture medium, will lead to the enhancement of the stability of bioengineered cartilage. However, it is still unclear how scaffold material influences the response of chondrocytes grown in the scaffolds to exogenous inflammatory stimuli, which may not be revealed by only studying chondrocyte growth under normal conditions. In this investigation, we focused on analyzing the differences in gene expression in 3D cultured chondrocytes under the treatment of pro-inflammatory cytokines, IL-1β and TNFα. We found that chondrocytes cultured in scaffolds of different materials (silk, collagen and PLA) showed varying responses in gene expression to pro-inflammatory cytokines, including matrix production and degradation, cell adhesion and cell death. Overall, silk and collagen scaffolds supported higher levels of cartilage matrix gene expression than PLA under IL-1β and TNFα treatments, which correlated with toluidine blue stainings that reflected the level of GAGs. Additionally, we compared chondrocyte gene expression with cell morphology and the biophysical properties of the scaffolds, such as release profiles of IL-1β and TNFα, and water uptake abilities. Together, these data strongly suggest that scaffolding is an important component of the microenvironment for chondrocytes and plays a significant role in chondrocyte homeostasis in an inflammatory environment.

4.1. Scaffolding material influences chondrocyte gene expression under inflammatory conditions

A number of studies have compared cartilage matrix production in engineered cartilage grown in scaffolds of different materials. In a recent comparison between silk and agarose hydrogels, Chao *et al.* found that cartilage constructs derived from these two materials yielded similar biochemical and biomechanical properties [72]. Work from Erickson *et al.* indicated that bovine articular chondrocytes (BACs) seeded in agarose gels had a higher level of GAG/DNA ratio than in scaffolds derived from hyaluronic acid (HA) and self-assembly peptides [73]. Consistently, Mouw *et al.* also reported that agarose gels supported a higher GAG/DNA ratio in BACs than alginate, collagen, fibrin or polyglycolic acid (PGA) [74]. In contrast, Hu *et al.* showed that PGA cartilage constructs contained more collagen than agarose constructs [75]. Another study compared polycaprolactone (PCL), poly-glycerol sebacate (PGS) and poly (1,8 octanediol-co-citrate) (POC) scaffolds, and found that POC supported the highest collagen II/collagen I ratio and higher aggrecan expression from porcine chondrocytes [76]. In addition to studying scaffolds of different materials, multiple groups also compared the properties of composite scaffolds that were derived from the same material, but with different modifications. It was found that various modifications of PCL and polyethylene glycol (PEG) scaffolds supported different GAG/DNA and collagen II levels [77, 78]. Together, these thorough studies indicated that scaffolding properties have significant impacts on cartilage gene expression. It is likely that electric charge, porosity and surface chemistry of the scaffolds all influence the cellular function of chondrocytes [73]. On the other hand, it is worth noting that these prior studies were performed under the non-pathological conditions. We believe that the challenge of inflammatory stimuli can further impact the role of scaffolding material on chondrocytes.

Here, we studied the effect of scaffoldings in the context of pro-inflammatory cytokine treatment, and evaluated porous scaffolds of silk, collagen and PLA, which were not directly compared in previous studies. We found that under control conditions, silk and collagen scaffolds supported higher levels of cartilage matrix deposition and expression of cartilage matrix genes collagen II, collagen IX and aggrecan than PLA scaffolds. In the presence of

NIH-PA Author Manuscript

NIH-PA Author Manuscript

NIH-PA Author Manuscript

IL-1β and TNFα, while all cartilage gene expression was significantly reduced, silk and collagen scaffolds still supported higher cartilage matrix levels.

Importantly however, in other instances, we found that chondrocytes' responses to inflammatory stimuli in different scaffolding materials may not be predicted from studying only non-inflammatory conditions. For example, in the case of MMP13 expression at day 16, while there was no difference among chondrocytes in different materials under control conditions, there was significantly higher MMP13 expression in the chondrocytes grown in PLA scaffolds than silk and collagen scaffolds in the presence of IL-1β and TNFα (Fig. 5). This result suggests that different scaffolding materials can elicit different responses to pro-inflammatory cytokines in the chondrocytes and that such effects can only be revealed when the cells are challenged with inflammatory stimuli. A recent investigation indicated that although there was no difference in cartilage matrix production in different PEG-modified scaffolds under static conditions, significant differences were observed when scaffolds were cultured under dynamic stimulation [78]. Thus, this investigation is consistent with the notion that scaffolding material influences the response to exogenous stimuli, including biochemical and biomechanical signals.

We have also observed that chondrocytes responded differently to the two different cytokines IL-1β and TNFα. In terms of ADAMTS4 expression, chondrocytes grown in silk scaffolds showed a significantly stronger response at day 8 to IL-1β than TNFα, while those grown in collagen and PLA scaffolds responded to IL-1β and TNFα equally. Furthermore, IL-1β is much more potent than TNFα in inducing MMP3 (day 16), MMP13 (day 8) and iNOS expression (day 16), while TNFα induces the expression of hypertrophic marker alkaline phosphatase (day 8) and cell death indicator caspase 8 (day 8 and day 16) more readily, suggesting that these two cytokines can activate different signaling pathways. Another group also noted the differential responses chondrocytes to IL-1β and TNFα when the cells were cultured as monolayers for up to three days, suggesting that TNFα was a stronger inducer of cell death as it activated the expression of both caspase 3 and 8 more strongly [79, 80]. Our data are consistent with this observation of caspase 8 expression; however, we found that IL-1β and TNFα similarly induced caspase 3 expression, a discrepancy possibly due to the differences between 2D and 3D culture systems. In addition to the differences in the activities of TNFα and IL-1β, we have also observed differential gene expression with respect to culture time. For example, although there was no difference in aggrecan expression in chondrocytes cultured in different scaffolds upon IL-1β and TNFα treatments at day 8, there were significant differences in the expression by day 16 (Fig. 2), thereby suggesting that different scaffolding materials may exhibit different kinetic profiles in regulating cartilage gene expression.

4.2. Comparison of chondrocyte behavior with biophysical properties of the scaffolds

Biomaterials have different physical and chemical characteristics such as surface roughness and material hydrophobicity that can affect cell attachment, cell shape and chondrocyte gene expression [20, 81]. Our histological and SEM analyses showed that chondrocytes in PLA scaffolds had a more spread-out, sheet-like structure. Correspondingly, cells grown in PLA scaffolds had significantly higher expression of cell adhesion molecule α1 integrin and the lowest amount of cartilage matrix deposition and gene expression than those grown in silk and collagen scaffolds. This is consistent with a report by Ronziere et al, in which inhibition of α1 integrin resulted in a more rounded cell morphology and enhanced collagen II expression in chondrocytes embedded in collagen gels [45].

In this study, we attempted to understand the mechanisms by which scaffolds influence the behavior of chondrocytes under inflammatory conditions. We reasoned that the rate of scaffolds to release cytokines would impact the local environment of the chondrocytes. Prior

NIH-PA Author Manuscript

NIH-PA Author Manuscript

NIH-PA Author Manuscript

studies, many aiming at targeted protein release, have analyzed the release profiles of BMP2, VEGF and IGF-I proteins from silk, collagen and PLA scaffolds [82-88]. However, the release of pro-inflammatory cytokines has not been extensively studied. Here, we show that silk, collagen and PLA scaffolds have different kinetics in releasing IL-1β and TNFα, thus proposing that different scaffolding materials may support different levels of pro-inflammatory cytokines in the chondrocytes' microenvironment. Regardless of the amount of cytokine loaded, silk scaffolds released IL-1β and TNFα at a much faster rate than collagen and PLA scaffolds. This suggests that silk material may not adsorb as much cytokines as collagen and PLA-based scaffolds do, which may provide chondrocytes with a more optimal microenvironment. Indeed, the faster cytokine release rate by silk is correlated with a higher level of cartilage matrix production in chondrocytes grown in silk scaffolds. Interestingly, while collagen scaffolds consistently released cytokines more slowly than PLA scaffolds, collagen scaffolds supported higher levels of matrix gene expression, suggesting that other factors are also involved. It is possible that collagen provides an additional biochemical regulation on chondrocyte behavior through its binding to integrins [89, 90].

Hydrophilicity of the scaffolding material might be an additional property that influences cartilage gene expression and matrix deposition. Previous studies have shown that the morphology and bulk hydrophilic/hydrophobic qualities of the scaffolds influence the rate of water uptake of the scaffolds and may affect the subsequent cell reaction to inflammatory stimuli [61-63]. Our data showed that silk and collagen scaffolds have higher water uptake abilities than PLA scaffolds, which is correlated with higher levels of cartilage matrix gene expression in chondrocytes cultured in silk and collagen scaffolds. Furthermore, chondrocytes in PLA scaffolds had a more flattened morphology and elevated α1 integrin expression, which may also be correlated with material hydrophobicity. Our result with these porous scaffolds is consistent with other analyses using PEG-based hydrogels as cartilage constructs, where swelling ratio positively correlated with collagen II and aggrecan expression [78, 91, 92]. Therefore, scaffold swelling ratio and water uptake property can be an additional physical property of the scaffolds that regulate cartilage gene expression under normal and inflammatory conditions.

In summary, our study constitutes one of the first steps toward understanding the contribution of scaffold material to inflammatory response. It clearly shows that scaffolding, as an important component of the chondrocyte microenvironment, plays a critical role in matrix production and destruction as well as cell death, especially under inflammatory conditions. These analyses prompted us to conclude that silk and collagen scaffolds are the most optimal scaffolds for supporting stable cartilage matrix production than PLA scaffolds, based on the following criteria: 1) higher level of cartilage matrix gene expression and matrix deposition; 2) lower levels of cartilage degradation enzymes; 3) cell morphology that resembles native cartilage cells; 4) lower retention of inflammatory cytokines; and 5) higher water uptake ability.

It will be interesting to determine how the other properties of scaffolding materials, such as porosity, rigidity, degradation rate, adhesion domains, local stiffness and surface chemistry, can regulate the response of chondrocytes to inflammatory stimuli [92-95]. In particular, we would like to determine whether seeding density could alter the influence of scaffolding material on chondrocyte gene expression, as a higher seeding density would be needed to generate cartilage constructs for clinical applications. It is also likely that other cell sources or cell types, such as mesenchymal stem cells, may exhibit differential responses to inflammatory cytokines when grown in scaffolds of different materials. Further biochemical and biophysical studies of the cartilage constructs will help us to understand the interaction of stem cells or chondrocytes with its niche or microenvironment. It is conceivable that

NIH-PA Author Manuscript

NIH-PA Author Manuscript

NIH-PA Author Manuscript

selecting the proper scaffolding material and optimizing its biophysical properties will aid in the engineering of more stable cartilage tissues.

5. Conclusions

In this study, the effect of scaffold materials on the response of chondrocytes to IL-1β and TNFα-mediated inflammatory stimuli was evaluated. Degradable porous scaffolds derived from silk, collagen and polylactic acid (PLA) had different surface characteristics as assayed by scanning electron microscopy. In the presence of IL-1β and TNFα, chondrocytes grown in different biomaterials yielded significant differences in the expression of genes associated with cartilage matrix production and degradation, cell adhesion and cell death. Chondrocytes grown in silk and collagen scaffolds exhibited higher levels of cartilage matrix gene expression than those in the PLA scaffolds, both in non-inflammatory and inflammatory conditions. On the other hand, while there was no difference in MMP13 expression among chondrocytes grown in different scaffolds under control conditions at the end of the culture period, there was significantly higher MMP13 expression in chondrocytes cultured in PLA scaffolds than in silk and collagen scaffolds in the presence of IL-1β and TNFα. Toluidine blue staining analysis confirmed our gene expression analyses and further demonstrated that different scaffolding materials supported different chondrocyte behaviors under inflammatory conditions. These effects may be related to the biophysical properties of scaffolding material, including the ability of the scaffolds to release pro-inflammatory cytokines and to uptake water. Therefore, scaffolding material plays an important role in regulating cellular response of chondrocytes and is a key component to consider in engineering stable and strong cartilage tissues in an inflammatory environment.

Supplementary Material

Refer to Web version on PubMed Central for supplementary material.

Acknowledgments

We are grateful to Catherine Linsenmayer and Lawrence Barry at Tufts imaging facility for help with the scanning electron microscopy. This work has been supported by grants to LZ and DLK from the NSF (CBET-0966920) and NIH (1R01AR059106-01A1, P41EB002520).

References

[1]. Bijlsma JW, Berenbaum F, Lafeber FP. Osteoarthritis: an update with relevance for clinical practice. Lancet. 2011; 377:2115–26. [PubMed: 21684382]

[2]. Clouet J, Vinatier C, Merceron C, Pot-vaucel M, Maugars Y, Weiss P, et al. From osteoarthritis treatments to future regenerative therapies for cartilage. Drug Discov Today. 2009; 14:913–25. [PubMed: 19651235]

[3]. Pelletier JP, Martel-Pelletier J, Abramson SB. Osteoarthritis, an inflammatory disease: potential implication for the selection of new therapeutic targets. Arthritis Rheum. 2001; 44:1237–47. [PubMed: 11407681]

[4]. Hunziker EB. Articular cartilage repair: problems and perspectives. Biorheology. 2000; 37:163–4. [PubMed: 10912188]

[5]. Chung C, Burdick JA. Engineering cartilage tissue. Adv Drug Deliv Rev. 2008; 60:243–62. [PubMed: 17976858]

[6]. Vinatier C, Bouffi C, Merceron C, Gordeladze J, Brondello JM, Jorgensen C, et al. Cartilage tissue engineering: towards a biomaterial-assisted mesenchymal stem cell therapy. Curr Stem Cell Res Ther. 2009; 4:318–29. [PubMed: 19804369]

[7]. Smith GD, Knutsen G, Richardson JB. A clinical review of cartilage repair techniques. J Bone Joint Surg Br. 2005; 87:445–9. [PubMed: 15795189]

NIH-PA Author Manuscript

NIH-PA Author Manuscript

NIH-PA Author Manuscript

[8]. Elder SH, Cooley A, Borazjani A, Sowell B, To H, Tran S. Production of Hyaline-Like Cartilage by Bone Marrow Mesenchymal Stem Cells in a Self-Assembly Model. Tissue Eng Part A. 2009

[9]. Glowacki J. In vitro engineering of cartilage. J Rehabil Res Dev. 2000; 37:171–7. [PubMed: 10850823]

[10]. Erggelet C, Kreuz PC, Mrosek EH, Schagemann JC, Lahm A, Ducommun PP, et al. Autologous chondrocyte implantation versus ACI using 3D-bioresorbable graft for the treatment of large full-thickness cartilage lesions of the knee. Arch Orthop Trauma Surg. 2010; 130:957–64. [PubMed: 19711090]

[11]. Schagemann JC, Erggelet C, Chung HW, Lahm A, Kurz H, Mrosek EH. Cell-laden and cell-free biopolymer hydrogel for the treatment of osteochondral defects in a sheep model. Tissue Eng Part A. 2009; 15:75–82. [PubMed: 18783325]

[12]. Siclari A, Mascaro G, Gentili C, Cancedda R, Boux E. A Cell-free Scaffold-based Cartilage Repair Provides Improved Function Hyaline-like Repair at One year. Clin Orthop Relat Res. 2011

[13]. Getgood A, Brooks R, Fortier L, Rushton N. Articular cartilage tissue engineering: today's research, tomorrow's practice? J Bone Joint Surg Br. 2009; 91:565–76. [PubMed: 19407287]

[14]. Ochi M, Uchio Y, Kawasaki K, Wakitani S, Iwasa J. Transplantation of cartilage-like tissue made by tissue engineering in the treatment of cartilage defects of the knee. J Bone Joint Surg Br. 2002; 84:571–8. [PubMed: 12043781]

[15]. Kuroda R, Ishida K, Matsumoto T, Akisue T, Fujioka H, Mizuno K, et al. Treatment of a full-thickness articular cartilage defect in the femoral condyle of an athlete with autologous bone-marrow stromal cells. Osteoarthritis Cartilage. 2007; 15:226–31. [PubMed: 17002893]

[16]. Amin AR, Dave M, Attur M, Abramson SB. COX-2, NO, and cartilage damage and repair. Curr Rheumatol Rep. 2000; 2:447–53. [PubMed: 11123096]

[17]. Lotz JC, Ulrich JA. Innervation, inflammation, and hypermobility may characterize pathologic disc degeneration: review of animal model data. J Bone Joint Surg Am. 2006; 88(Suppl 2):76–82. [PubMed: 16595449]

[18]. Steinert AF, Ghivizzani SC, Rethwilm A, Tuan RS, Evans CH, Noth U. Major biological obstacles for persistent cell-based regeneration of articular cartilage. Arthritis Res Ther. 2007; 9:213. [PubMed: 17561986]

[19]. Schlegel W, Nurnberger S, Hombauer M, Albrecht C, Vecsei V, Marlovits S. Scaffold-dependent differentiation of human articular chondrocytes. Int J Mol Med. 2008; 22:691–9. [PubMed: 18949392]

[20]. Boyan BD, Hummert TW, Dean DD, Schwartz Z. Role of material surfaces in regulating bone and cartilage cell response. Biomaterials. 1996; 17:137–46. [PubMed: 8624390]

[21]. Albrecht C, Tichy B, Nurnberger S, Hosiner S, Zak L, Aldrian S, et al. Gene expression and cell differentiation in matrix-associated chondrocyte transplantation grafts: a comparative study. Osteoarthritis and cartilage/OARS, Osteoarthritis Research Society. 2011; 19:1219–27.

[22]. Kim UJ, Park J, Kim HJ, Wada M, Kaplan DL. Three-dimensional aqueous-derived biomaterial scaffolds from silk fibroin. Biomaterials. 2005; 26:2775–85. [PubMed: 15585282]

[23]. Chu CR, Monosov AZ, Amiel D. In situ assessment of cell viability within biodegradable polylactic acid polymer matrices. Biomaterials. 1995; 16:1381–4. [PubMed: 8590764]

[24]. Ju YM, Park K, Son JS, Kim JJ, Rhie JW, Han DK. Beneficial effect of hydrophilized porous polymer scaffolds in tissue-engineered cartilage formation. J Biomed Mater Res B Appl Biomater. 2008; 85:252–60. [PubMed: 17973245]

[25]. Meinel L, Fajardo R, Hofmann S, Langer R, Chen J, Snyder B, et al. Silk implants for the healing of critical size bone defects. Bone. 2005; 37:688–98. [PubMed: 16140599]

[26]. Glowacki J, Mizuno S. Collagen scaffolds for tissue engineering. Biopolymers. 2008; 89:338–44. [PubMed: 17941007]

[27]. Kim HJ, Kim UJ, Vunjak-Novakovic G, Min BH, Kaplan DL. Influence of macroporous protein scaffolds on bone tissue engineering from bone marrow stem cells. Biomaterials. 2005; 26:4442–52. [PubMed: 15701373]

NIH-PA Author Manuscript

NIH-PA Author Manuscript

NIH-PA Author Manuscript

[28]. Meinel L, Hofmann S, Karageorgiou V, Kirker-Head C, McCool J, Gronowicz G, et al. The inflammatory responses to silk films in vitro and in vivo. Biomaterials. 2005; 26:147–55. [PubMed: 15207461]

[29]. Altman GH, Diaz F, Jakuba C, Calabro T, Horan RL, Chen J, et al. Silk-based biomaterials. Biomaterials. 2003; 24:401–16. [PubMed: 12423595]

[30]. Wang Y, Blasioli DJ, Kim HJ, Kim HS, Kaplan DL. Cartilage tissue engineering with silk scaffolds and human articular chondrocytes. Biomaterials. 2006; 27:4434–42. [PubMed: 16677707]

[31]. Wang Y, Kim HJ, Vunjak-Novakovic G, Kaplan DL. Stem cell-based tissue engineering with silk biomaterials. Biomaterials. 2006; 27:6064–82. [PubMed: 16890988]

[32]. Wang Y, Kim UJ, Blasioli DJ, Kim HJ, Kaplan DL. In vitro cartilage tissue engineering with 3D porous aqueous-derived silk scaffolds and mesenchymal stem cells. Biomaterials. 2005; 26:7082–94. [PubMed: 15985292]

[33]. Nazarov R, Jin HJ, Kaplan DL. Porous 3-D scaffolds from regenerated silk fibroin. Biomacromolecules. 2004; 5:718–26. [PubMed: 15132652]

[34]. Abramoff M, Magelhaes P, Ram S. Image processing with ImageJ. Biophotonics International. 2004; 11:36–42.

[35]. Girish V, Vijayalakshmi A. Affordable image analysis using NIH Image/ImageJ. Indian J Cancer. 2004; 41:47. [PubMed: 15105580]

[36]. Karageorgiou V, Kaplan D. Porosity of 3D biomaterial scaffolds and osteogenesis. Biomaterials. 2005; 26:5474–91. [PubMed: 15860204]

[37]. Nishiguchi S, Kato H, Neo M, Oka M, Kim HM, Kokubo T, et al. Alkali- and heat-treated porous titanium for orthopedic implants. Journal of biomedical materials research. 2001; 54:198–208. [PubMed: 11093179]

[38]. Park SN, Park JC, Kim HO, Song MJ, Suh H. Characterization of porous collagen/hyaluronic acid scaffold modified by 1-ethyl-3-(3-dimethylaminopropyl)carbodiimide cross-linking. Biomaterials. 2002; 23:1205–12. [PubMed: 11791924]

[39]. Bruckschen B, Steitz H, Buzug TM, Tille C, Leukers B, Irsen S. Comparing different porosity measurement methods for characterisation of 3D printed bone replacement scaffolds. Biomed Tech (Berl). 2005; 50:1609–10.

[40]. Mauck RL, Seyhan SL, Ateshian GA, Hung CT. Influence of seeding density and dynamic deformational loading on the developing structure/function relationships of chondrocyte-seeded agarose hydrogels. Ann Biomed Eng. 2002; 30:1046–56. [PubMed: 12449765]

[41]. Cairns D, Lee P, Uchimura T, Seufert C, Kwon H, Zeng L. The role of muscle cells in regulating cartilage matrix production. J Orthop Res. 2010; 28:529–36. [PubMed: 19813241]

[42]. Stockwell, RA. Biology of Cartilage Cells (Biological Structure and Function Books). Cambridge University Press; 1979.

[43]. Cake MA, Read RA, Guillou B, Ghosh P. Modification of articular cartilage and subchondral bone pathology in an ovine meniscectomy model of osteoarthritis by avocado and soya unsaponifiables (ASU). Osteoarthritis and cartilage/OARS, Osteoarthritis Research Society. 2000; 8:404–11.

[44]. Scheuner G, Hutschenreiter J. Metachromasia, double refraction and dichroism caused by Toluidine Blue reaction. Prog Histochem Cytochem. 1975; 7:1–73. author's transl. [PubMed: 62370]

[45]. Ronziere MC, Aubert-Foucher E, Gouttenoire J, Bernaud J, Herbage D, Mallein-Gerin F. Integrin alpha1beta1 mediates collagen induction of MMP-13 expression in MC615 chondrocytes. Biochim Biophys Acta. 2005; 1746:55–64. [PubMed: 16198011]

[46]. Kiani C, Chen L, Wu YJ, Yee AJ, Yang BB. Structure and function of aggrecan. Cell Res. 2002; 12:19–32. [PubMed: 11942407]

[47]. Chandran PL, Horkay F. Aggrecan, an unusual polyelectrolyte: Review of solution behavior and physiological implications. Acta Biomater. 2012; 8:3–12. [PubMed: 21884828]

[48]. Bell DM, Leung KK, Wheatley SC, Ng LJ, Zhou S, Ling KW, et al. SOX9 directly regulates the type-II collagen gene. Nat Genet. 1997; 16:174–8. [PubMed: 9171829]

NIH-PA Author Manuscript

NIH-PA Author Manuscript

NIH-PA Author Manuscript

[49]. Bi W, Deng JM, Zhang Z, Behringer RR, de Crombrugghe B. Sox9 is required for cartilage formation. Nat Genet. 1999; 22:85–9. [PubMed: 10319868]

[50]. Burrage PS, Mix KS, Brinckerhoff CE. Matrix metalloproteinases: role in arthritis. Front Biosci. 2006; 11:529–43. [PubMed: 16146751]

[51]. Goessler UR, Bieback K, Bugert P, Heller T, Sadick H, Hormann K, et al. In vitro analysis of integrin expression during chondrogenic differentiation of mesenchymal stem cells and chondrocytes upon dedifferentiation in cell culture. Int J Mol Med. 2006; 17:301–7. [PubMed: 16391830]

[52]. Lee JW, Kim YH, Park KD, Jee KS, Shin JW, Hahn SB. Importance of integrin beta1-mediated cell adhesion on biodegradable polymers under serum depletion in mesenchymal stem cells and chondrocytes. Biomaterials. 2004; 25:1901–9. [PubMed: 14738854]

[53]. Shintani Y, Fukumoto Y, Chaika N, Svoboda R, Wheelock MJ, Johnson KR. Collagen I-mediated up-regulation of N-cadherin requires cooperative signals from integrins and discoidin domain receptor 1. J Cell Biol. 2008; 180:1277–89. [PubMed: 18362184]

[54]. Nakazora S, Matsumine A, Iino T, Hasegawa M, Kinoshita A, Uemura K, et al. The cleavage of N-cadherin is essential for chondrocyte differentiation. Biochem Biophys Res Commun. 2010; 400:493–9. [PubMed: 20735983]

[55]. DeLise AM, Tuan RS. Alterations in the spatiotemporal expression pattern and function of N-cadherin inhibit cellular condensation and chondrogenesis of limb mesenchymal cells in vitro. J Cell Biochem. 2002; 87:342–59. [PubMed: 12397616]

[56]. Delise AM, Tuan RS. Analysis of N-cadherin function in limb mesenchymal chondrogenesis in vitro. Dev Dyn. 2002; 225:195–204. [PubMed: 12242719]

[57]. Tuli R, Tuli S, Nandi S, Huang X, Manner PA, Hozack WJ, et al. Transforming growth factor-beta-mediated chondrogenesis of human mesenchymal progenitor cells involves N-cadherin and mitogen-activated protein kinase and Wnt signaling cross-talk. J Biol Chem. 2003; 278:41227–36. [PubMed: 12893825]

[58]. Woods A, Wang G, Beier F. Regulation of chondrocyte differentiation by the actin cytoskeleton and adhesive interactions. J Cell Physiol. 2007; 213:1–8. [PubMed: 17492773]

[59]. Woods A, Wang G, Dupuis H, Shao Z, Beier F. Rac1 signaling stimulates N-cadherin expression, mesenchymal condensation, and chondrogenesis. J Biol Chem. 2007; 282:23500–8. [PubMed: 17573353]

[60]. Goldring SR, Goldring MB. The role of cytokines in cartilage matrix degeneration in osteoarthritis. Clin Orthop Relat Res. 2004; S27:36.

[61]. Miot S, Woodfield T, Daniels AU, Suetterlin R, Peterschmitt I, Heberer M, et al. Effects of scaffold composition and architecture on human nasal chondrocyte redifferentiation and cartilaginous matrix deposition. Biomaterials. 2005; 26:2479–89. [PubMed: 15585250]

[62]. Mohan N, Nair PD, Tabata Y. A 3D biodegradable protein based matrix for cartilage tissue engineering and stem cell differentiation to cartilage. J Mater Sci Mater Med. 2009; 20(Suppl 1):S49–60. [PubMed: 18560767]

[63]. Arima Y, Iwata H. Effect of wettability and surface functional groups on protein adsorption and cell adhesion using well-defined mixed self-assembled monolayers. Biomaterials. 2007; 28:3074–82. [PubMed: 17428532]

[64]. Dinerman AA, Cappello J, Ghandehari H, Hoag SW. Swelling behavior of a genetically engineered silk-elastinlike protein polymer hydrogel. Biomaterials. 2002; 23:4203–10. [PubMed: 12194523]

[65]. Lima EG, Tan AR, Tai T, Bian L, Stoker AM, Ateshian GA, et al. Differences in Interleukin-1 Response between Engineered and Native Cartilage. Tissue Eng Part A. 2008

[66]. Sun L, Wang X, Kaplan DL. A 3D cartilage - inflammatory cell culture system for the modeling of human osteoarthritis. Biomaterials. 2011; 32:5581–9. [PubMed: 21565399]

[67]. Mastbergen SC, Lafeber FP, Bijlsma JW. Selective COX-2 inhibition prevents proinflammatory cytokine-induced cartilage damage. Rheumatology (Oxford). 2002; 41:801–8. [PubMed: 12096231]

[68]. Montaseri A, Busch F, Mobasheri A, Buhrmann C, Aldinger C, Rad JS, et al. IGF-1 and PDGF-bb suppress IL-1beta-induced cartilage degradation through down-regulation of NF-kappaB

NIH-PA Author Manuscript

NIH-PA Author Manuscript

NIH-PA Author Manuscript

signaling: involvement of Src/PI-3K/AKT pathway. PLoS ONE. 2011; 6:e28663. [PubMed: 22194879]

[69]. Kafienah W, Al-Fayez F, Hollander AP, Barker MD. Inhibition of cartilage degradation: a combined tissue engineering and gene therapy approach. Arthritis and rheumatism. 2003; 48:709–18. [PubMed: 12632424]

[70]. Lima EG, Tan AR, Tai T, Marra KG, Defail A, Ateshian GA, et al. Genipin enhances the mechanical properties of tissue-engineered cartilage and protects against inflammatory degradation when used as a medium supplement. J Biomed Mater Res A. 2008

[71]. Lima EG, Tan AR, Tai T, Bian L, Ateshian GA, Cook JL, et al. Physiologic deformational loading does not counteract the catabolic effects of interleukin-1 in long-term culture of chondrocyte-seeded agarose constructs. Journal of biomechanics. 2008; 41:3253–9. [PubMed: 18823628]

[72]. Chao PH, Yodmuang S, Wang X, Sun L, Kaplan DL, Vunjak-Novakovic G. Silk hydrogel for cartilage tissue engineering. J Biomed Mater Res B Appl Biomater. 2010; 95:84–90. [PubMed: 20725950]

[73]. Erickson IE, Huang AH, Sengupta S, Kestle S, Burdick JA, Mauck RL. Macromer density influences mesenchymal stem cell chondrogenesis and maturation in photocrosslinked hyaluronic acid hydrogels. Osteoarthritis Cartilage. 2009; 17:1639–48. [PubMed: 19631307]

[74]. Mouw JK, Case ND, Guldberg RE, Plaas AH, Levenston ME. Variations in matrix composition and GAG fine structure among scaffolds for cartilage tissue engineering. Osteoarthritis Cartilage. 2005; 13:828–36. [PubMed: 16006153]

[75]. Hu JC, Athanasiou KA. Low-density cultures of bovine chondrocytes: effects of scaffold material and culture system. Biomaterials. 2005; 26:2001–12. [PubMed: 15576174]

[76]. Jeong CG, Hollister SJ. A comparison of the influence of material on in vitro cartilage tissue engineering with PCL, PGS, and POC 3D scaffold architecture seeded with chondrocytes. Biomaterials. 2010; 31:4304–12. [PubMed: 20219243]

[77]. Schagemann JC, Kurz H, Casper ME, Stone JS, Dadsetan M, Yu-Long S, et al. The effect of scaffold composition on the early structural characteristics of chondrocytes and expression of adhesion molecules. Biomaterials. 2010

[78]. Appelman TP, Mizrahi J, Elisseeff JH, Seliktar D. The influence of biological motifs and dynamic mechanical stimulation in hydrogel scaffold systems on the phenotype of chondrocytes. Biomaterials. 2011; 32:1508–16. [PubMed: 21093907]

[79]. Carames B, Lopez-Armada MJ, Cillero-Pastor B, Lires-Dean M, Vaamonde C, Galdo F, et al. Differential effects of tumor necrosis factor-alpha and interleukin-1beta on cell death in human articular chondrocytes. Osteoarthritis Cartilage. 2008; 16:715–22. [PubMed: 18054255]

[80]. Lopez-Armada MJ, Carames B, Lires-Dean M, Cillero-Pastor B, Ruiz-Romero C, Galdo F, et al. Cytokines, tumor necrosis factor-alpha and interleukin-1beta, differentially regulate apoptosis in osteoarthritis cultured human chondrocytes. Osteoarthritis Cartilage. 2006; 14:660–9. [PubMed: 16492401]

[81]. Choi CK, Breckenridge MT, Chen CS. Engineered materials and the cellular microenvironment: a strengthening interface between cell biology and bioengineering. Trends Cell Biol. 2010; 20:705–14. [PubMed: 20965727]

[82]. Wang Y, Zhang L, Hu M, Wen W, Xiao H, Niu Y. Effect of chondroitin sulfate modification on rhBMP-2 release kinetics from collagen delivery system. Journal of Biomedical Materials Research Part A. 2009; 92A:693–701.

[83]. Kleinheinz J, Jung S, Wermker K, Fischer C, Joos U. Release kinetics of VEGF165 from a collagen matrix and structural matrix changes in a circulation model. Head Face Med. 2010; 6:17. [PubMed: 20642842]

[84]. Karageorgiou V, Tomkins M, Fajardo R, Meinel L, Snyder B, Wade K, et al. Porous silk fibroin 3-D scaffolds for delivery of bone morphogenetic protein-2 in vitro and in vivo. J Biomed Mater Res A. 2006; 78:324–34. [PubMed: 16637042]

[85]. Uebersax L, Merkle HP, Meinel L. Insulin-like growth factor I releasing silk fibroin scaffolds induce chondrogenic differentiation of human mesenchymal stem cells. J Control Release. 2008; 127:12–21. [PubMed: 18280603]

NIH-PA Author Manuscript

NIH-PA Author Manuscript

NIH-PA Author Manuscript

[86]. Kanczler JM, Barry J, Ginty P, Howdle SM, Shakesheff KM, Oreffo RO. Supercritical carbon dioxide generated vascular endothelial growth factor encapsulated poly(DL-lactic acid) scaffolds induce angiogenesis in vitro. Biochem Biophys Res Commun. 2007; 352:135–41. [PubMed: 17112464]

[87]. Niu X, Feng Q, Wang M, Guo X, Zheng Q. Porous nano-HA/collagen/PLLA scaffold containing chitosan microspheres for controlled delivery of synthetic peptide derived from BMP-2. J Control Release. 2009; 134:111–7. [PubMed: 19100794]

[88]. Mullen LM, Best SM, Brooks RA, Ghose S, Gwynne JH, Wardale J, et al. Binding and release characteristics of insulin-like growth factor-1 from a collagen-glycosaminoglycan scaffold. Tissue Eng Part C Methods. 2010; 16:1439–48. [PubMed: 20388039]

[89]. Schuman L, Buma P, Versleyen D, de Man B, van der Kraan PM, Berg WB, et al. Chondrocyte behaviour within different types of collagen gel in vitro. Biomaterials. 1995; 16:809–14. [PubMed: 7492712]

[90]. Heinegard D. Proteoglycans and more--from molecules to biology. Int J Exp Pathol. 2009; 90:575–86. [PubMed: 19958398]

[91]. Park JS, Woo DG, Sun BK, Chung HM, Im SJ, Choi YM, et al. In vitro and in vivo test of PEG/PCL-based hydrogel scaffold for cell delivery application. J Control Release. 2007; 124:51–9. [PubMed: 17904679]

[92]. Park H, Guo X, Temenoff JS, Tabata Y, Caplan AI, Kasper FK, et al. Effect of swelling ratio of injectable hydrogel composites on chondrogenic differentiation of encapsulated rabbit marrow mesenchymal stem cells in vitro. Biomacromolecules. 2009; 10:541–6. [PubMed: 19173557]

[93]. Karande TS, Ong JL, Agrawal CM. Diffusion in musculoskeletal tissue engineering scaffolds: design issues related to porosity, permeability, architecture, and nutrient mixing. Ann Biomed Eng. 2004; 32:1728–43. [PubMed: 15675684]

[94]. Raghunath J, Rollo J, Sales KM, Butler PE, Seifalian AM. Biomaterials and scaffold design: key to tissue-engineering cartilage. Biotechnol Appl Biochem. 2007; 46:73–84. [PubMed: 17227284]

[95]. Tee SY, Fu J, Chen CS, Janmey PA. Cell shape and substrate rigidity both regulate cell stiffness. Biophys J. 2011; 100:L25–7. [PubMed: 21354386]

NIH-PA Author Manuscript
NIH-PA Author Manuscript
NIH-PA Author Manuscript

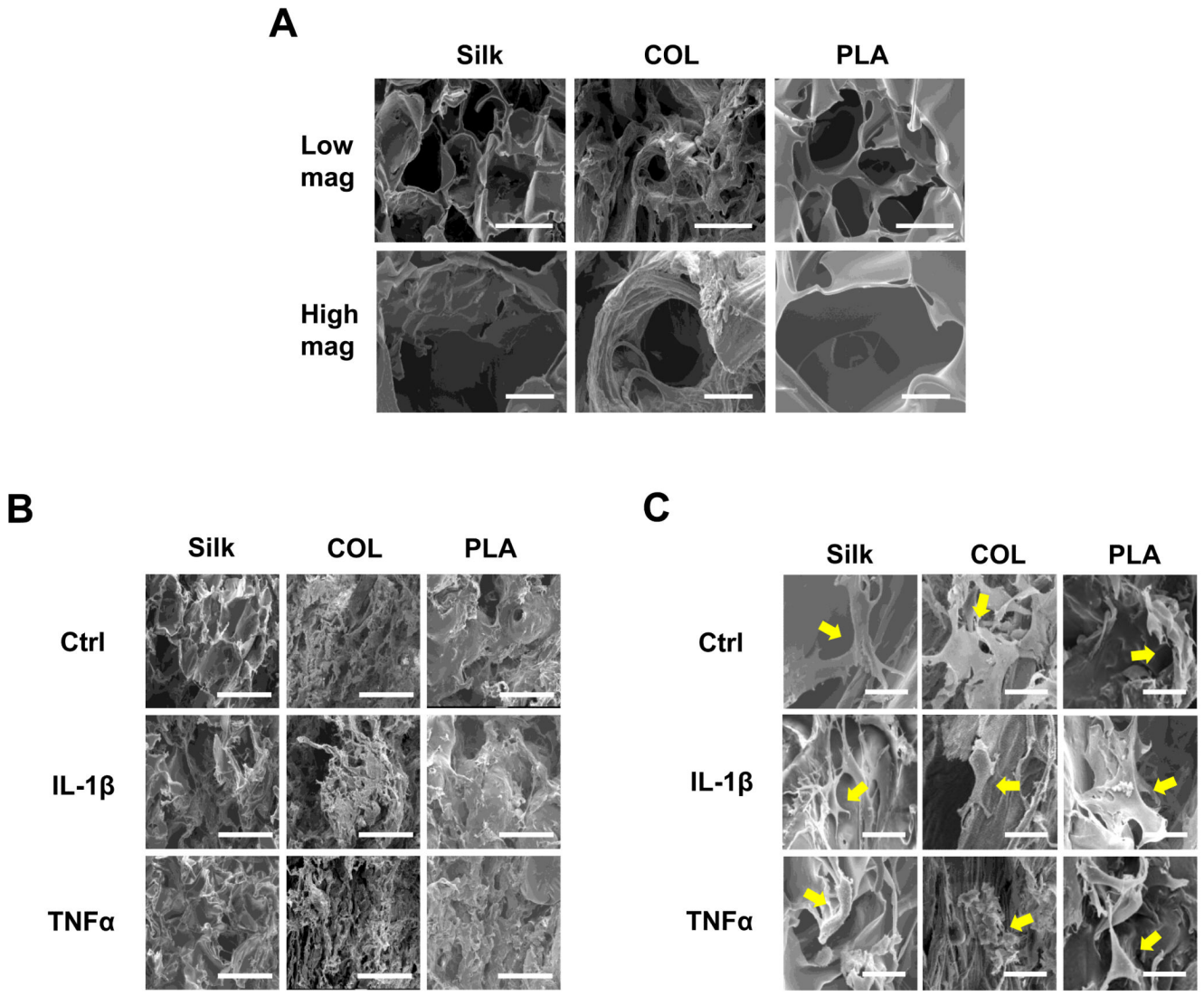

Fig. 1. Morphological characterization of scaffolds and chondrocytes by scanning electron microscopy (SEM)

(A) SEM micrographs of cell-free silk, collagen (COL), and polylactic-acid (PLA) scaffolds. Top panels: low magnification, scale bar: 200μm. Bottom panel, high magnification, scale bar: 50μm. **(B)** Low magnification images of chondrocytes inside the scaffolds after 16 days of culture. Scale bar: 200μm. **(C)** High magnification images of chondrocytes inside the scaffolds after 16 days of culture (see arrows). Scale bar: 25μm. The treatments are: Ctrl (no cytokines added), IL-1β (10ng/ml), and TNFα (10ng/ml).

NIH-PA Author Manuscript
NIH-PA Author Manuscript
NIH-PA Author Manuscript

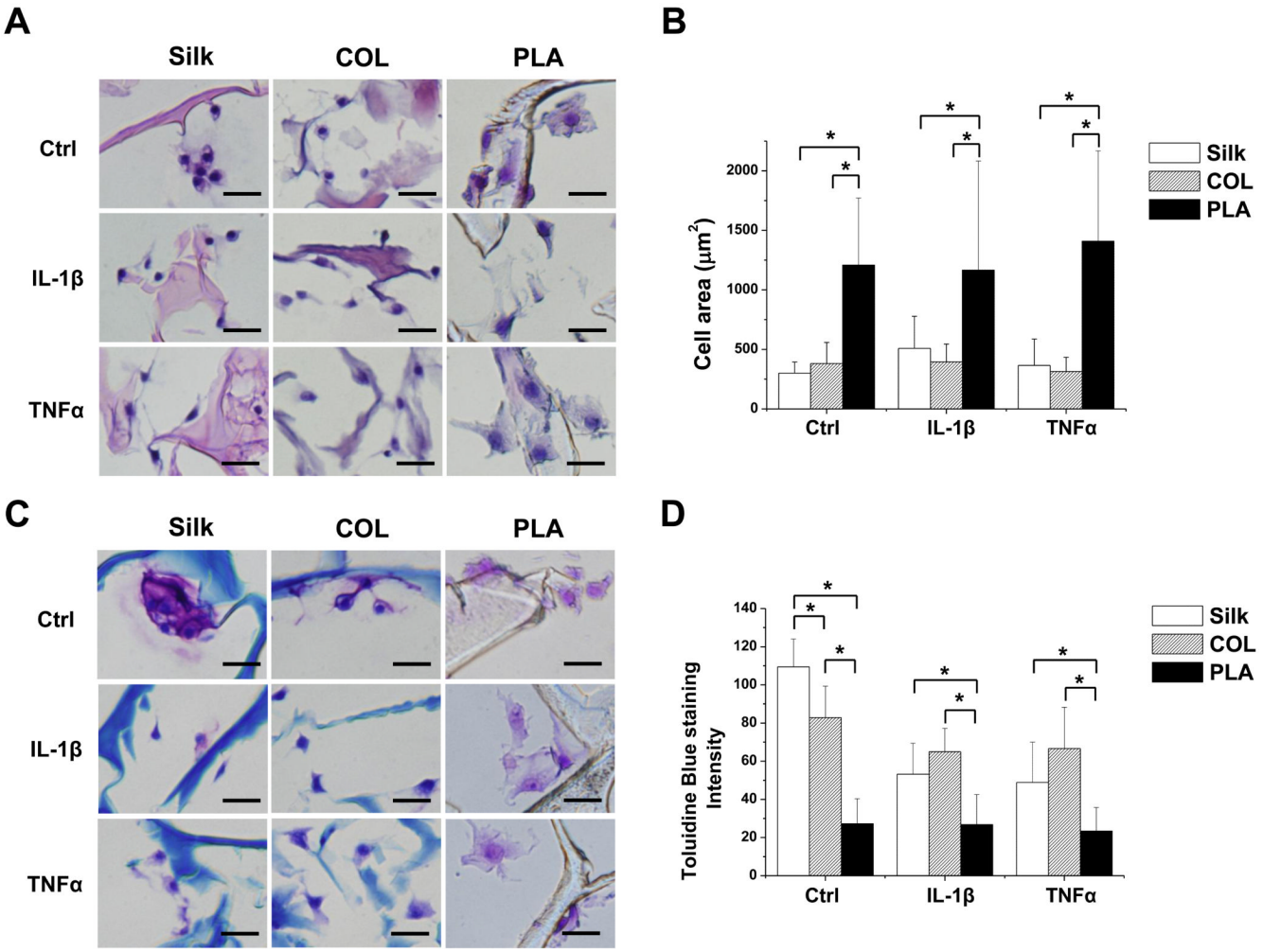

Fig. 2. Histological analyses of chondrocytes grown in silk, collagen and PLA scaffolds

A. H&E staining images. **B.** Average area (μm^2) occupied by individual chondrocytes was quantified by using Image J. **C.** Toluidine blue staining images. **D.** Average toluidine blue staining per cell, as quantified using Image J analysis. Scale bars: 25μm. Data present mean ± SD. *p<0.05.

NIH-PA Author Manuscript
NIH-PA Author Manuscript
NIH-PA Author Manuscript

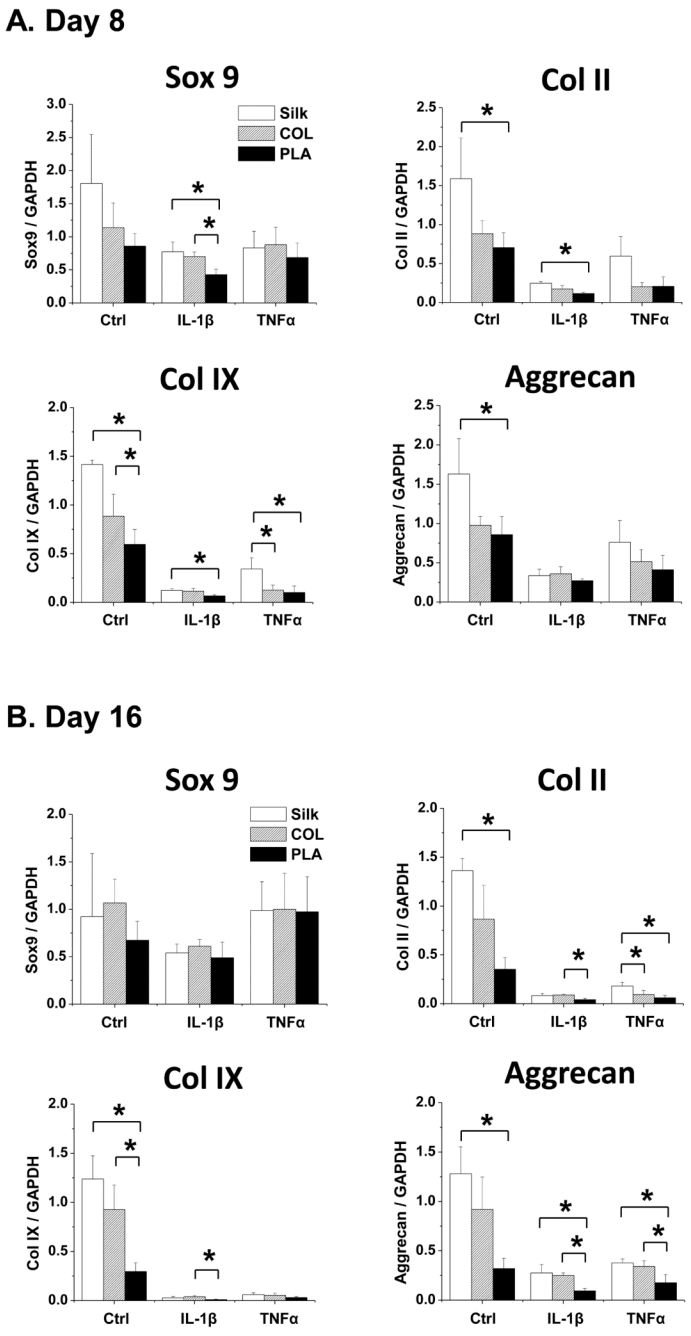

Fig. 3. mRNA analysis of genes associated with cartilage matrix production in chondrocytes cultured in silk, collagen and PLA scaffolds

qRT-PCR analysis of Sox9, collagen (Col II), collagen IX (Col IX), and aggrecan in control (Ctrl), IL-1β treated (10ng/ml) or TNFα treated (10ng/ml) samples. For each treatment, results from three independent samples are shown. **(A)** Gene expression from Day 8 cultures. **(B)** Gene expression from Day 16 cultures. All gene expression levels were normalized to GAPDH. Data present mean ± SD. *p<0.05.

NIH-PA Author Manuscript
NIH-PA Author Manuscript
NIH-PA Author Manuscript

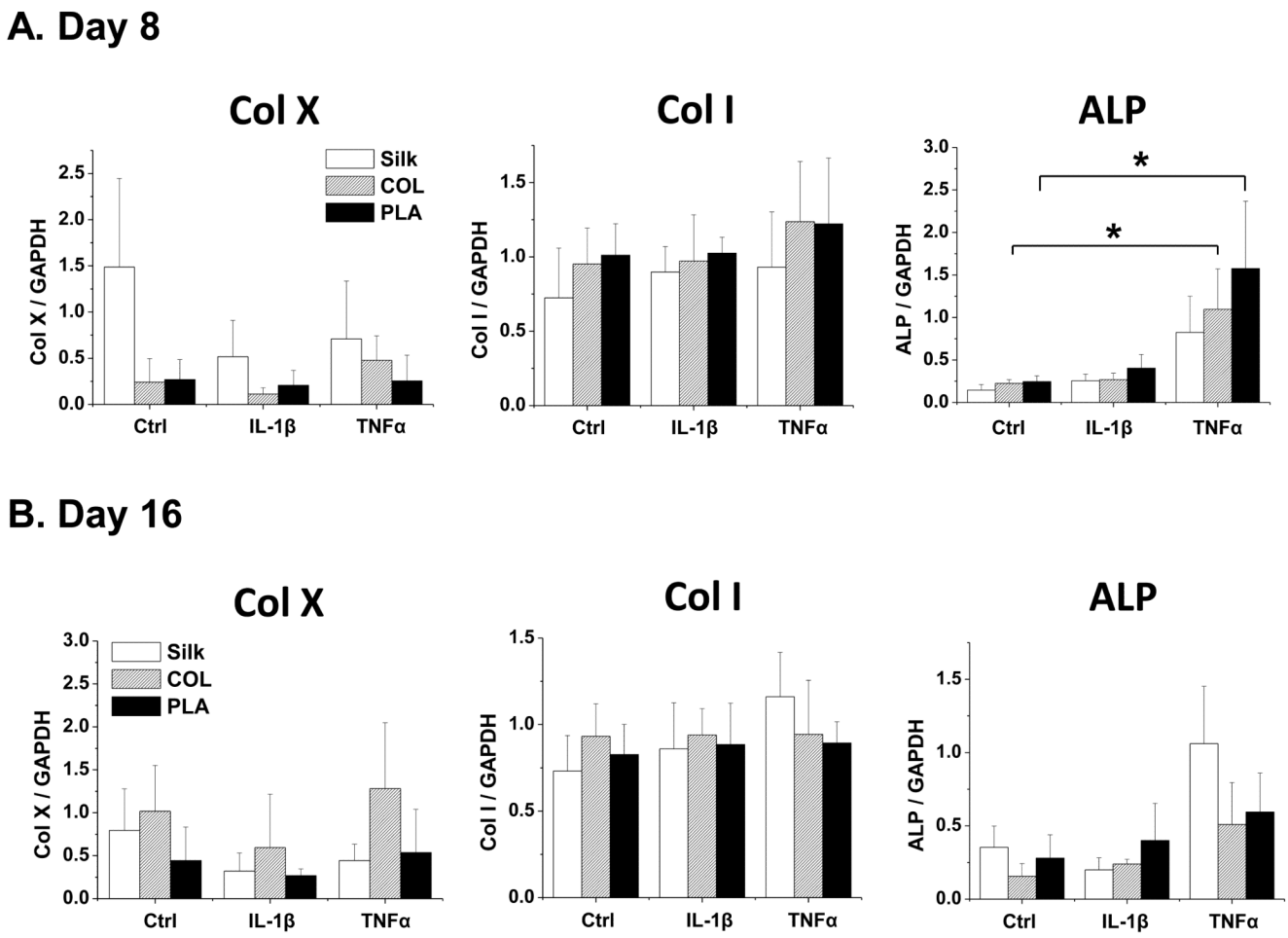

Fig. 4. Gene expression analysis of chondrocyte hypertrophy and dedifferentiation markers in chondrocytes cultured in silk, collagen and PLA scaffolds

The expression of hypertrophy markers collagen X (Col X) and alkaline phosphatase (ALP), and dedifferentiation marker collagen I (Col I) in Ctrl (no cytokine treatment) or IL-1β (10ng/ml) and TNFα (10ng/ml) treated samples were evaluated. For each treatment, results from three independent samples are shown. **(A)** Gene expression from Day 8 cultures. **(B)** Gene expression from Day 16 cultures. All gene expression levels were normalized to GAPDH. Data present mean ± SD. *p<0.05.

NIH-PA Author Manuscript
NIH-PA Author Manuscript
NIH-PA Author Manuscript

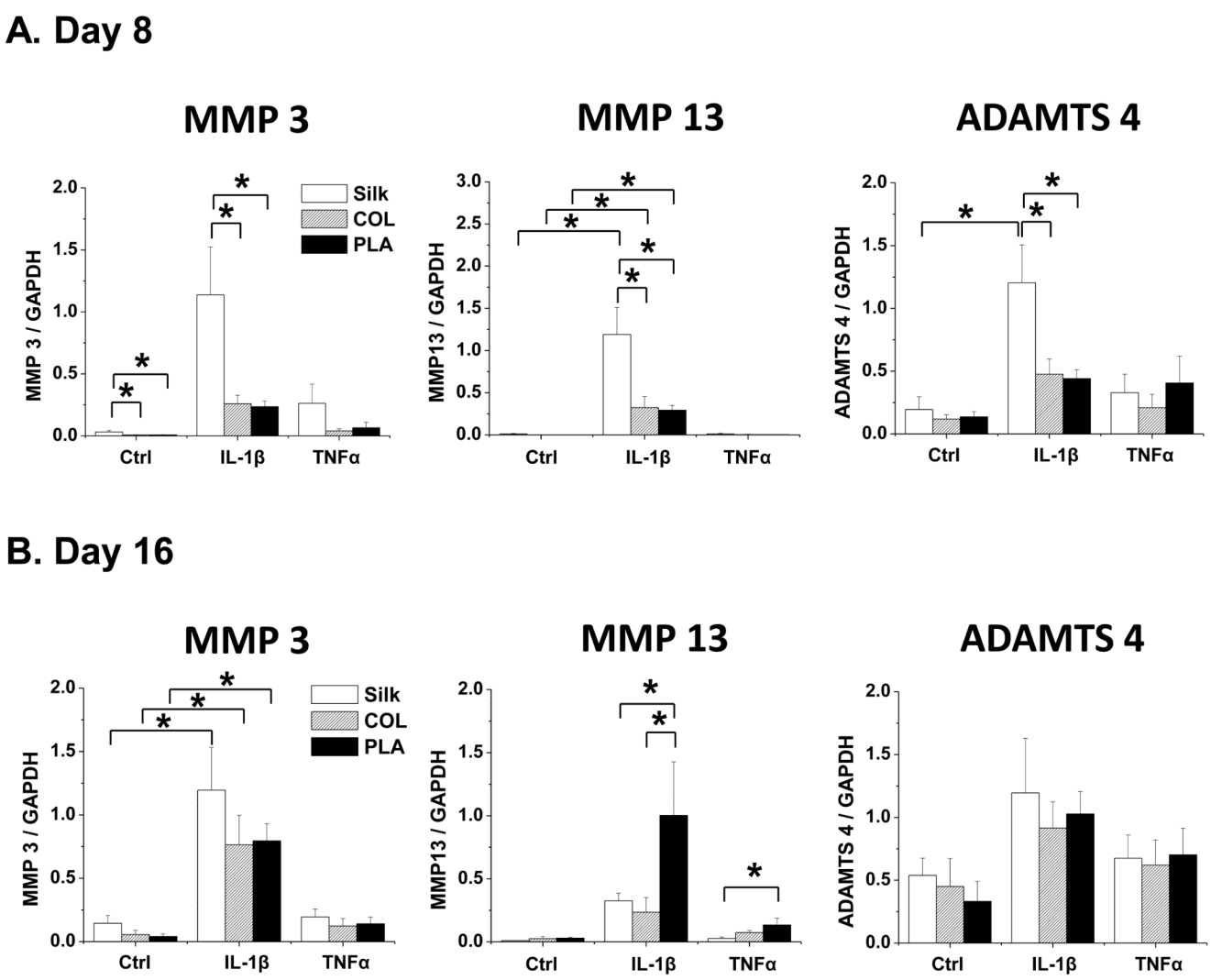

Fig. 5. Gene expression analysis of cartilage degradation enzymes in chondrocytes cultured in silk, collagen and PLA scaffolds

The expression of cartilage-degrading enzymes MMP3, MMP13, and ADAMTS4 in Ctrl (no cytokine treatment) or IL-1β (10ng/ml) and TNFα (10ng/ml) treated samples were evaluated. For each treatment, results from three independent samples are shown. **(A)** Gene expression from Day 8 cultures. **(B)** Gene expression from Day 16 cultures. All gene expression levels were normalized to GAPDH. Data present mean ± SD. *p<0.05.

NIH-PA Author Manuscript
NIH-PA Author Manuscript
NIH-PA Author Manuscript

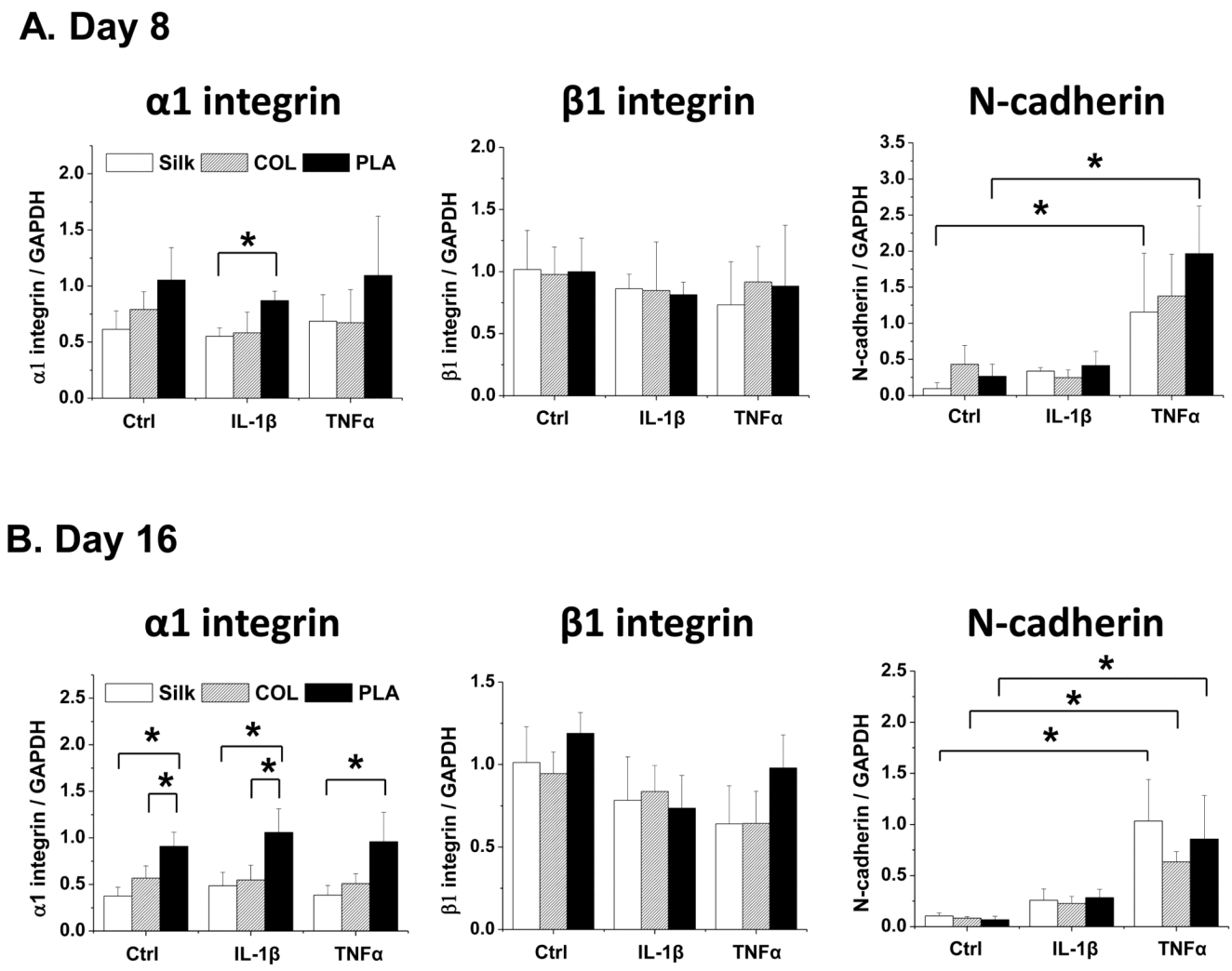

Fig. 6. Gene expression analysis of cell adhesion molecules in chondrocytes cultured in silk, collagen and PLA scaffolds

The expression of α1 integrin, β1 integrin, and N-cadherin in Ctrl (no cytokine treatment) or IL-1β (10ng/ml) and TNFα (10ng/ml) treated samples were evaluated. For each treatment, results from three independent samples are shown. **(A)** Gene expression from Day 8 cultures. **(B)** Gene expression from Day 16 cultures. All gene expression levels were normalized to GAPDH. Data present mean ± SD. *p<0.05.

NIH-PA Author Manuscript
NIH-PA Author Manuscript
NIH-PA Author Manuscript

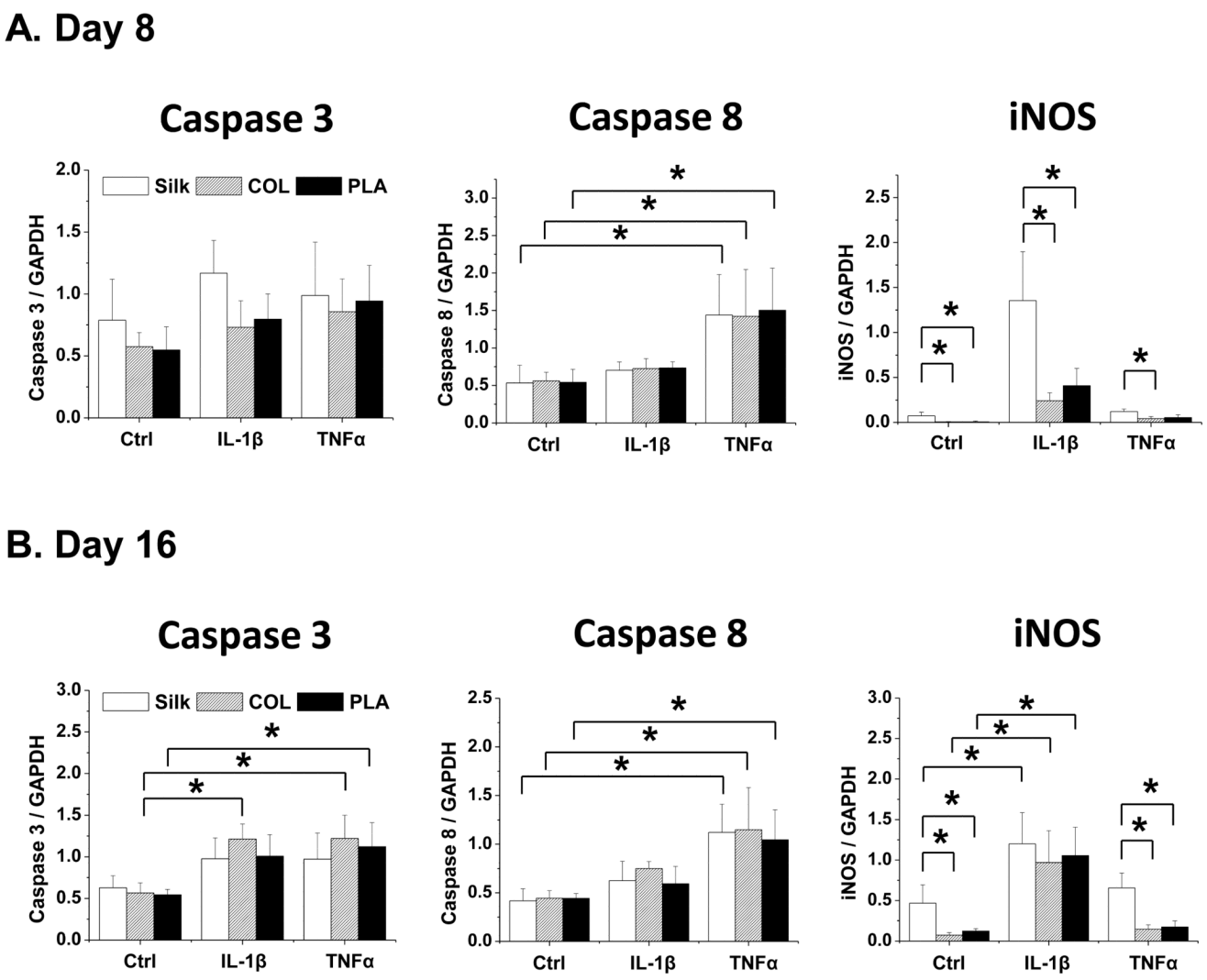

Fig. 7. Gene expression analysis of apoptosis-related factors in chondrocytes cultured in silk, collagen and PLA scaffolds

The expression of caspase 3, caspase 8, and iNOS in Ctrl (no cytokine treatment) or IL-1β (10ng/ml) and TNFα (10ng/ml) treated samples were evaluated. For each treatment, results from three independent samples are shown. **(A)** Results from Day 8 cultures. **(B)** Results from Day 16 cultures. All gene expression levels were normalized to GAPDH. Data present mean ± SD. *p<0.05.

NIH-PA Author Manuscript
NIH-PA Author Manuscript
NIH-PA Author Manuscript

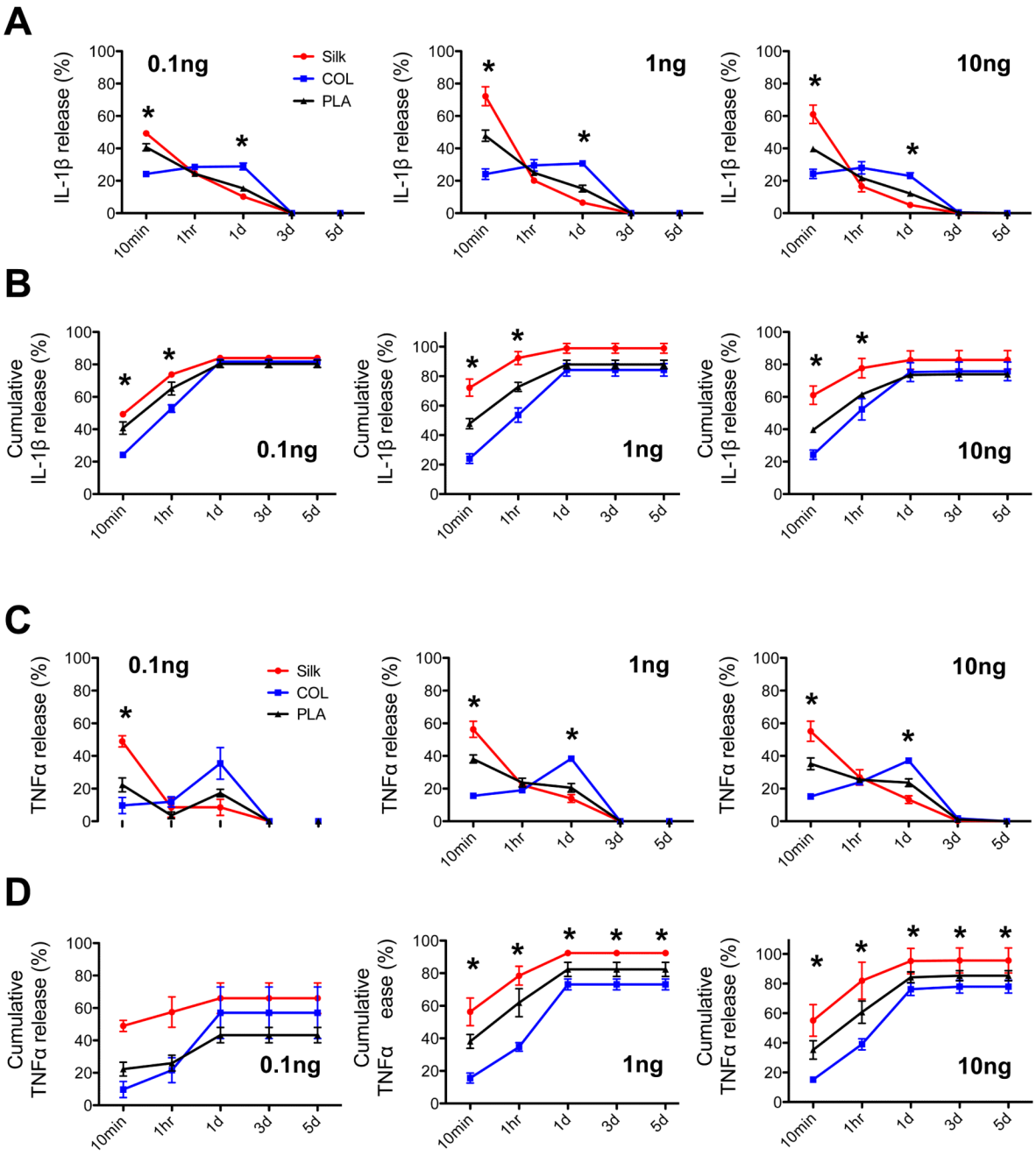

Fig. 8. Evaluation of cytokine release kinetics of silk, collagen and PLA scaffolds

Three different amounts of pro-inflammatory cytokines IL-1β or TNFα (0.1, 1 and 10ng) were loaded onto empty scaffolds of silk, collagen (COL), polylactic-acid (PLA). ELISA was used to verify the initial loading amount and to evaluate the amount of cytokines leached into the medium at 5 different time points: 10min, 1hr, 1 day, 3 days and 5 days. **(A)** Percent release of IL-1β from scaffolds at each time point. **(B)** Analysis of IL-1β cumulative release from the scaffolds. **(C)** Percent release of TNFα from scaffolds at each time point. **(D)** Analysis of TNFα cumulative release from scaffolds. Data present mean ± SD. Statistical analysis of the data was determined by two-way ANOVA. *p<0.05.

NIH-PA Author Manuscript

NIH-PA Author Manuscript

NIH-PA Author Manuscript

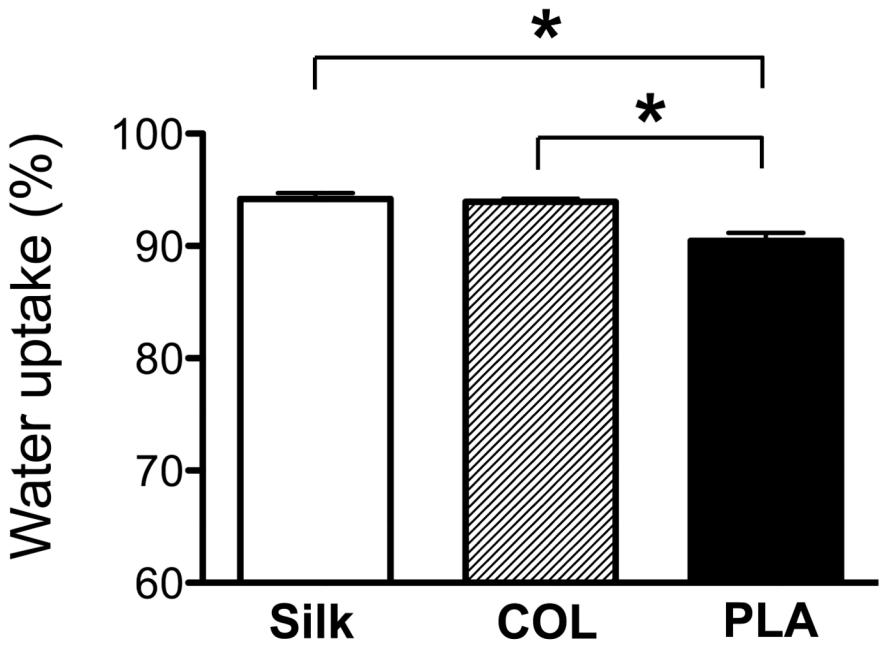

Fig. 9. Analysis of water uptake properties of silk, collagen and PLA scaffolds

Percentage of water uptake in the scaffolds was determined. Statistical analysis of the data was determined by one-way ANOVA. Data present mean ± SD. *p<0.05.